

A VISION-BASED FUZZY EXPERT SYSTEM FOR THE SURVEILLANCE AND DIAGNOSIS OF HYDRODAMS USING UNDERWATER COLOR IMAGE ANALYSIS

Abstract: *Surveillance of hydro plants represents a serious environmental problem. Limited access to upstream areas of hydro-dams makes their visual inspection difficult. However few attempts to build computer vision systems for upstream dam walls monitoring and diagnosis are currently reported; this artificial vision application area is on its beginning. In this paper we propose a novel solution towards the automation of underwater hydro-dams monitoring and diagnosis, based on the visual examination of color underwater images of the upstream dam walls acquired with the use of an underwater robot vehicle. Whereas the traditional methods require the human expert to visually examine the underwater images (a time-consuming and tiring task), the solution presented here reduces significantly the need for a human expert examination. This goal has been achieved by developing an image analysis subsystem specific to underwater dam wall examination, designing a fuzzy expert subsystem for the upstream dam wall diagnosis and combining the two subsystems into a complete vision-based fuzzy expert system for a specific diagnosis task of the dam walls.*

Keywords: *computer vision; color image segmentation; underwater image analysis; fuzzy expert system; hydro-dam visual diagnosis*

1. Introduction

Surveillance and monitoring of the hydro dams represent a serious environmental and technical problem. Some tasks of the hydro dam inspection process, especially the examination of the dam walls, require their visual inspection. However, limited access to certain areas, especially the upstream side of a dam, makes their inspection process difficult. Recently, computer vision techniques are considered a cutting-edge technology, promising for the underwater surveillance of the wet side of the dam. Among the systems based on the computer vision techniques for dam inspection, a first achievement was reported by Hydro-Québec, Canada [1]; an underwater robot vehicle (URV) is used for the inspection of upstream dam walls and other structures in hostile environments. The URV possesses vision capabilities, using two color video-cameras to produce 3D images of the underwater dam walls. A similar system, based on a remote operated vehicle (ROV) with vision capabilities provided by a color video-camera, is the one presented in [2]. In this work, the acquired underwater images of the upstream dam walls were processed to obtain the dam wall mosaic. Another system making use of artificial vision for dam inspection is the one reported in [3]. This system proposes a method based on image analysis in the visual domain, using surface images, to measure the water level of the dam, by capturing images around the water surface.

As these works show, so far the emphasise was mainly on the hardware design of the URV and on the system of video cameras used for accurate image acquisition. Less progress has been done in developing image analysis algorithms to automatically analyse the acquired images of the upstream dam walls, thus helping the human in the visual dam monitoring and diagnosis task. However the importance of vision in underwater robots vehicles as well as the interest in automated underwater image analysis for various surveillance and monitoring tasks [4,5] is more and more often admitted. Therefore we consider that soon the computer vision-based expert systems for the monitoring and diagnosis of the hydro-dams will become a powerful new application of the artificial vision. The vision-based fuzzy expert system presented in this paper, designed for the diagnosis of the upstream face of a hydro-dam, represents such a novel application of a fuzzy expert system based on underwater image analysis techniques.

2. Overview of the proposed vision-based fuzzy expert system

2.1. The tasks of the proposed system

In the general framework of upstream hydro-dam walls visual examination for monitoring and diagnosis, a specific task is to examine the metal sliding bars that support the protective shield. These

metal sliding bars consist from flat metal bar green pieces, fixed in screws on the protective shield, illustrated in Figure 1.

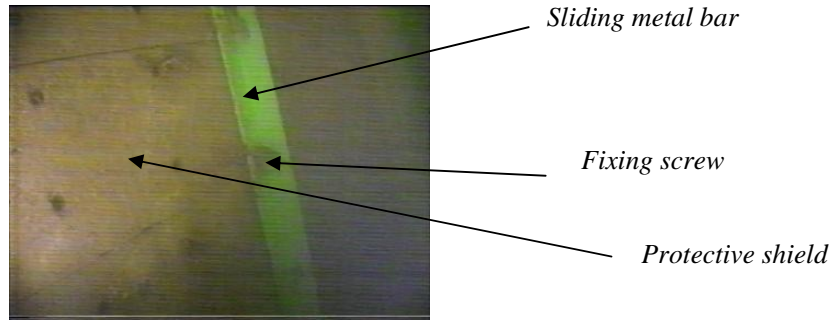


Figure 1. Underwater image of the upstream dam wall with sliding metal bar

The protective shield is a layer made of concrete slices (with pressure equalization holes) placed in front of the concrete walls of the dam on the upstream side in order to prevent rocks and stumps (brought in by the river after the winter from the mountain sides) to hit and possibly damage the dam walls. Therefore evaluating the status of the protective shield and of the flat metal sliding bars that support the protective shield is very important in the surveillance and diagnosis of the hydro-dam.

Human experts usually evaluate the shield and its metal sliding bars visually. The two visual examinations are considered as separate tasks; in the following we address only the second task: the visual examination of the metal sliding bars supporting the shield. The examination is done considering the following set of information about the status of the sliding bars, collected from the human experts in the field:

- integrity check of the sliding bar: the bar can have portions corroded by the water, or a displacement between two ends of the pieces of the bar;
- pieces of algae or rust on the screws that fix the bar on the shield; this is illustrated in Figure 2(a), and in time it can lead to a faulty operation of the shield.

Also in the underwater images of the sliding bars, we may have obstacles in front of the bars, as tree branches, that make the sliding bar not visible for the visual examination, as illustrated in Figure 2(b). In this case, no information can be collected about the status of the bar in that portion.

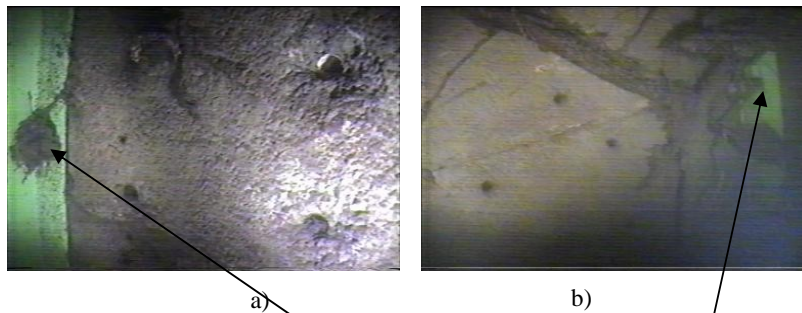


Figure 2. Underwater images with sliding metal bars, in which:
a) a piece of algae is present on a fixing screw; b) the sliding bar is almost completely occluded by obstacles (tree branches)

However, only a subset of the underwater images of the upstream dam walls will contain metal sliding bars. On the other hand, especially when using an URV system, the number of images acquired in the inspection process is very large (on the order of 10000 images/session), even for a part of the dam. This renders the human visual inspection a very time-consuming (and tiring) process. An automated image analysis system, combined with an expert system to point the user directly to the images that contain possibly damaged portions of metal sliding bars and give information about the degree of damage in a linguistic fashion, can ease very much the visual inspection task. This is purpose of the system presented here.

2.2. The block diagram of the proposed system

In order to perform an automated visual investigation of the sliding metal bars in the color underwater images of the upstream dam walls and to provide as result of the investigation linguistic information about the successive parts of the sliding metal bar, two components need to be included in our computer vision system:

- a) An **image analysis component**, which will be responsible for:
 - (i) the rough localization of the sliding metal bar in the underwater image (determining and separating the so-called region of interest (ROI); the region of interest will be the only image part used for further processing and data extraction)
 - (ii) the segmentation of the region of interest into areas belonging to the object of interest (i.e. to the sliding metal bar), areas belonging to the background (i.e. the shield) and areas corresponding to obstacles (i.e. tree branches, algae, rocks etc.)
 - (iii) accurate separation of the areas corresponding to the object of interest (the sliding metal bar) and any other areas in the region of interest (background or obstacles) and quantitative description of the object of interest; this stage will provide the data needed by the expert system in order to decide about the status of the sliding metal bar and give a linguistic evaluation of this status.
- b) An **expert system component to diagnose** the metal sliding bar. Based on the information received from the image analysis component and on the knowledge base “learned” from human experts visual, it will provide its diagnostic about the status of the bar (according to the issues of interest mentioned in subsection 2.1) in the form of some linguistic labels.

The principled block-diagram of the proposed vision-based expert system is presented in Figure 3.

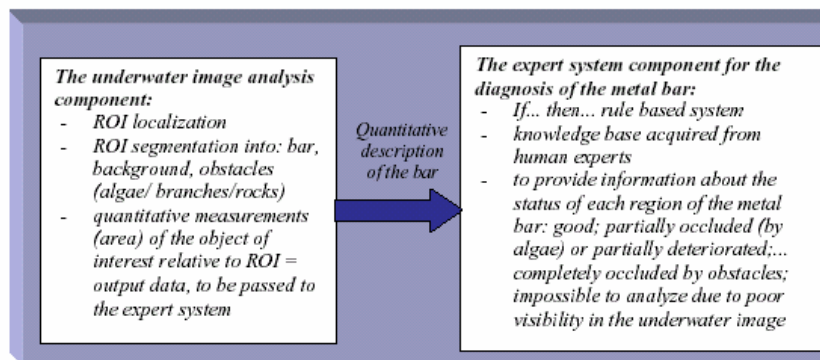


Figure 3. The block-diagram of the proposed vision-based expert system for the diagnosis of sliding metal bars in underwater images of the upstream dam walls

3. The image analysis component

As briefly explained in the previous section, this component is responsible for extracting useful information about the object of interest (the sliding metal green bar) from the current underwater image to be processed. Underwater image analysis is in general a much more difficult task than the analysis of color images in the visible domain [5]. The difficulty in processing the underwater dam images comes from their particularities, namely: low visibility, variable illumination, low contrast and blurring. Some of these particularities (as the variation of illumination and blurring) are partially introduced by the acquisition system (in most of the cases – an Underwater Robot Vehicle (URV) equipped with a video-camera).

Therefore the suitable image analysis techniques must be carefully selected, depending on the specific application to be solved. There are no general methods from the large class of image processing algorithms to be “universally” applied to underwater image analysis, but rather, in the design of an underwater image analysis system, experiments must be performed in respect to the best combination of algorithms, processing parameters and feature spaces to find the solution that gives the desired results.

Another consequence of the poor quality of underwater images is that using only the luminance component for the image analysis is not sufficient. No information loss is affordable in the case of these images; therefore the use of color information is essential for good processing results. This

principle is also employed in the system designed here, especially since the color is a highly discriminative feature for the object of interest in our application: the sliding metal bars, of green color, as opposite to the shield, algae and tree branches, which have a gray-to-brown or gray-to-green color.

As in general in the case of image analysis systems for not very good quality images [6,7], dividing the image analysis process in several steps is benefic. As the first step we should first roughly select a region of interest from the image, containing the object of interest. Then we will process and analyze only the selected region of interest, to:

- (a) segment as accurate as possible the object of interest from the other parts of the region of interest; depending on the image at hand, this segmentation can also be a rather difficult task, and it might require more than one step (algorithm).
- (b) provide some quantitative description of the object of interest, in our case – some area measurements of the object of interest – the sliding metal bar.

3.1. Region of interest localization

This step can be seen as an image pre-processing one. During the region of interest localization, we define our objective as to select from the currently analyzed underwater image the smallest possible rectangular region that contains completely the sliding metal bar portion present in the image, with no loss of sliding metal bar areas.

To do that in an easy and fast fashion, we make use of a rough color discriminative feature between the bar and the background (i.e. the shield). Since the sliding metal bar has dominant green color whereas the concrete shield has dominant gray-to-brown color, then considering the representation of the color image in the (R,G,B) space, the color difference between the green component and the red component, $R-G$, will be a good discriminative between the bar and the shield as:

- (a) it will have a large value for the sliding metal bar (large G, very small R)
- (b) it will have a small value for the concrete shield (comparable values of G and R) and also for the tree branches and algae.

Of course, in the real case of the underwater images considered, the discriminative power of $G-R$ will not be as good as it should ideally, and this is due to the green-like illumination in the water. This can be noticed in the $G-R$ image presented in Figure 4(b) for the original image in Figure 4(a).

However the $G-R$ discriminator becomes strong enough for defining the image of interest around the sliding bar if we perform a histogram stretching of the resulting $G-R$ image. Then the image from Figure 4(b) leads to the image in Figure 4(c), where the difference $G-R$ values for the sliding bar are indeed significantly larger than the difference $G-R$ values for the other objects in the scene, allowing the localization of the ROI.

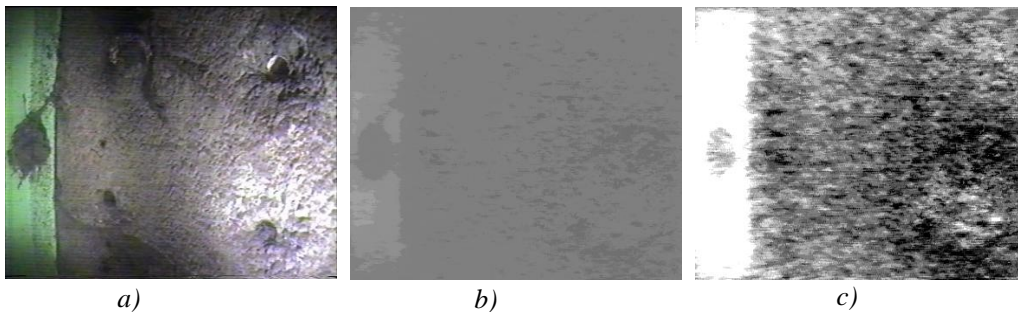


Figure 4. Illustration of the discriminative character of the $G-R$ color difference component for the sliding metal bar: a) the original underwater image – the bar is not clearly separable in respect to all areas of the shield; b) the $G-R$ image, without histogram stretching; c) the $G-R$ image, after histogram stretching – the bar is clearly separable from the rest of the scene

Even with this additional histogram processing, there are cases of very poor underwater images when parasitic image regions, with large values of $G-R$ outside the sliding bar, appear. To reject these parasitic image regions from ROI, we apply a simple algorithm in which:

- (a) We first threshold the image with a value T_{G-R} that separates in the stretched histogram the very large values of G-R from the small values G-R. Thus we obtain a binary image comprising white “candidate regions” to the sliding bar category on a black background
- (b) We measure the area in pixels of each candidate region and keep as real sliding bar regions only those whose area is at least 90% from the largest candidate region area

Afterwards, the minimum rectangle containing the regions decided to belong to the sliding metal bar represents the ROI and is selected from the original underwater image for further processing. The ROI resulting for the original image in Figure 4(a) as output of the ROI localization stage is presented in Figure 5.



Figure 5. The resulting ROI for the original image in Figure 4(a) at the output of the ROI localization stage

3.2. Color segmentation of the region of interest

The output of the previous step is a sub-image (denoted as ROI) that contains not only the object of interest, but also some (small) regions belonging to the shield and possibly obstacles in the neighborhood of the object of interest. Therefore in order to describe the status of the object of interest, in our case the sliding metal bar, we must perform a segmentation of the ROI into (at least) two classes: one class comprising the image regions belonging to the sliding metal bar and the other class comprising regions from the shield and obstacles (tree branches, algae).

Even though the image to be segmented in this stage has a much simpler content than the entire underwater image used for analysis (since it is just a sub-image in which the main object is the sliding metal bar), the segmentation is not an easy task, due to the aforementioned particularities of the color underwater image (low contrast, poor illumination, variable illumination, water reflections, blurring).

As in the previous stage, we consider the use of color for segmentation, since the color of the sliding metal bar is the most discriminative feature from the other parts in the ROI. However our attempts to separate the sliding metal bar through color segmentation applied globally on the entire ROI lead to poor separation results of the sliding metal bar from the other parts of the ROI. Therefore we consider a further split of the ROI into 10 horizontal slices, of equal width, and applying a color image segmentation algorithm in each slice. Actually we consider this decomposition strategy benefic from other two points of view as well:

- (a) it allows the expert system to indicate with higher accuracy to the user the damaged/partially occluded by obstacles areas of the sliding metal bar;
- (b) it keeps the segmentation complexity on a low level, since the data set to be simultaneously processed (i.e. the number of pixels) is 10 times smaller than in the global segmentation case.

- **The 3-class color fuzzy c-means segmentation stage of the color underwater ROI**

A widely used segmentation algorithm, especially when the images are to be segmented at pixel level, with good results for noisy and blurred images [8,9] is fuzzy c-means [10]. One of the advantages of fuzzy c-means in color image segmentation comes from its ability to segment (classify) vector data; this allows us to completely represent each pixel by the 3 color components. The data set to be segmented in each slice is the set of pixel colors in the slice. We examined experimentally, on 10 images with different statistics, the suitability of color representation in different spaces for segmentation: (R,G,B), (H,L,S), (Y,U,V). If we use the standard form of fuzzy c-means, with Euclidean distance function [10], then the most suitable feature space for representing the color according to this distance between the colors is the (R,G,B) space.

The number of classes for fuzzy c-means segmentation was also experimentally selected, considering as candidates two values: C=2 – corresponding to the segmentation of slice pixels into “sliding metal bar” and “other regions”; C=3 – corresponding to the segmentation of slice pixels into “sliding metal bar”, “shield” and “other”. The value C=2 proves unsuitable for a reliable segmentation; in this case, some of the experiments run on the 10 images mentioned above show an incorrect assignment of some regions of the sliding metal bar to the “other regions” class and vice-

versa. However, $C=3$ gives an accurate enough segmentation result. Therefore the fuzzy c-means segmentation of each slice in the ROI was performed in the (R,G,B) space with the Euclidean distance in $C=3$ classes.

The fuzzy c-means segmentation result is illustrated in Figure 6(b) for the original image in Figure 6(a). Examining this segmentation result, one can notice two unwanted but expectable aspects in the segmented image:

(a) Incomplete segmentation at slice level: that is, there are slices in the segmented ROI where the sliding metal bar is represented by two different classes from the total of three (the classes being represented each one through a different color). This could be expected as long as we chose to employ a 3-class segmentation and taking into account the local lighting variability in the underwater image.

(b) From one slice to another, the color encoding the class that represents the sliding metal bar is different. This is the direct consequence of the independent segmentation of each of the 10 horizontal slices by fuzzy c-means and also of the local variability of the lighting as well as its piecewise greenish nuance, that renders the proper separation of the pixels belonging to the green sliding metal bar even more difficult.

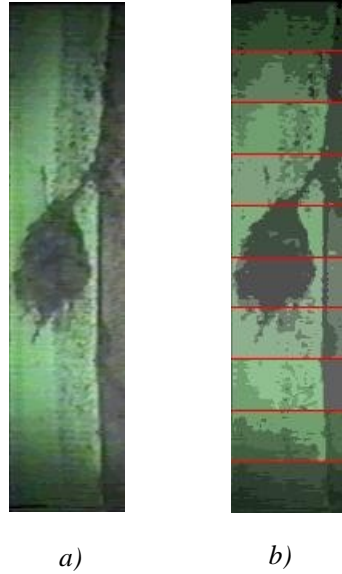


Figure 6. (a) the region of interest for an underwater color image with a sliding bar; (b) the result of color fuzzy c-means segmentation in the (R,G,B) space applied on each horizontal slice

In order to obtain a complete segmentation of the ROI pixels into sliding metal bar (object of interest in our application) as opposed to other parts of the image, we must then employ a second processing stage on the fuzzy c-means segmented image, to merge the regions belonging to the bar. This is again performed at slice level since we will use a slice-level diagnosis of the bar, and is described in the following.

- **The fuzzy if-then rule based segmentation of the fuzzy c-means segmented color ROI in bar vs. non-bar**

In order to obtain a complete segmentation of the ROI slices into only two categories: sliding metal bar or other objects (i.e. shield, obstacles) we chose to consider again (as in the ROI localization case) simple discriminative features based on the value of the green component of the pixels. This time the sub-image to be processed contains much simpler information than the original, since each slice has only three possible pixel colors.

Two discriminative features have been selected to decide whether to assign a color (therefore a pixel) to the class “sliding metal bar” or “not sliding metal bar”:

- the relative value of the green component of the color in the fuzzy c-means segmented slice, reported to the maximum value of the green component among the pixels in the current slice;
- the absolute value of the G-R color difference of the color in the fuzzy c-means segmented slice.

Denoting the current slice in the ROI by k , $k=1,2,\dots,10$, and indicating one of the colors in the slice by the index i , $i=1,2,3$, we denote and define the two above mentioned discriminative features considered for the 2-class complete segmentation of each slice by $GRel_{ik}$ and $GDifR_{ik}$, where:

$$GRel_{ik} = \frac{\max_{i=1}^3 G_{ik} - G_{ik}}{\max_{i=1}^3 G_{ik}}, \quad \forall k = 1,2,\dots,10, i = 1,2,3 \quad (1)$$

$$GDifR_{ik} = G_{ik} - R_{ik}, \forall k = 1,2,\dots,10, i = 1,2,3 \quad (2)$$

To use these features for the class assignment of each fuzzy c-means segmented slice pixels, we must find the rules describing the values of $(GRel_{ik}, GDifR_{ik})$ for each class. To do that we build a set of 10 training underwater images with different statistics, all containing the sliding metal bar. In every training image we apply the ROI selection step, the decomposition of ROI in 10 slices and the color fuzzy c-means segmentation of each slice. This will lead to a set of 10 images \times 10 slices = 100 training sub-images in which we compute the discriminative features $GRel_{ik}$, $GDifR_{ik}$ given by equations (1) and (2). A human observer is asked to classify on each of the 100 fuzzy c-means segmented slices each of the three colors resulting after segmentation into “sliding metal bar”, “not sliding metal bar” or “can’t decide”, based on the visual examination of the fuzzy c-means segmented slices.

Examining the human observer decision on the set of 100 slices, we notice several cases when the answer is “can’t decide”. This situations mostly occur in the regions where the visibility in the underwater image is poor. An example is given in Table 1, where a portion of the human decision is given, for the image in Figure 6(b).

Table 1. The human decision on the correct classification of slice colors in the fuzzy c-means segmented slice (illustration): “x”= sliding bar; “-” = not sliding bar; “x-” = can’t decide

GMax-G1	GMax-G2	GMax-G3	G1-R1	G2-R2	G3-R3	(x)/(-)/(x-)	(x)/(-)/(x-)	(x)/(-)/(x-)	GMax
0	24	76	20	12	0	x	-	-	76
0	32	68	28	20	8	x	x-	-	124
0	24	80	36	36	12	x	x	-	156
0	40	84	40	24	12	x	x-	-	168
0	88	60	36	12	8	x	-	-	172
0	84	48	20	8	4	x	-	-	172

The observation that even the human expert is unable to visually classify in a crisp manner the three colors resulting after the fuzzy c-means segmentation of each slice into “sliding bar” or “not sliding bar” leads to the conclusion that a fuzzy classification is more suitable than a crisp one for the final segmentation of the slices in the ROI. Therefore, based on the discriminative features given by the equations (1) and (2), we aim to derive a number of fuzzy sets and fuzzy if-then rules for the 2-class classification problem. To do that, we plot the pre-computed features $GRel_{ik}$ and $GDifR_{ik}$, $i=1,2,3$ and $k=1,2,\dots,10$ for all the 10 images considered for training, for which the labeling is available from the human expert. Each point described by $(GRel, GDifR)$ (100 points available) is represented by a different symbol, according to its label, as shown in Figure 7.

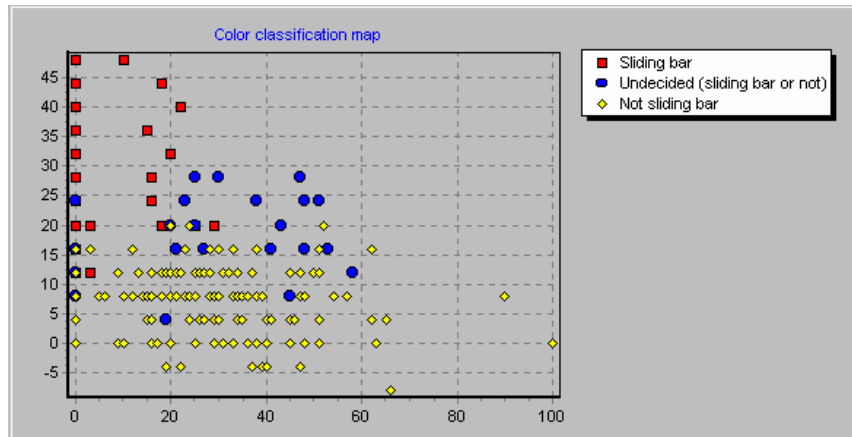


Figure 7. The graphical display in the $GRel$ (x-axis) and $GDifR$ (y-axis) of the resulting colours after the fuzzy c-means segmentation of the 10 training images, with their assigned labels as: sliding bar, not sliding bar and undecided, provided by a human expert.

Based on the resulting plot on which the data separability can be examined, we define the minimal number of fuzzy patches to extract the fuzzy sets parameters used in the if-then rule classification (this is a common strategy for deriving fuzzy sets from numerical data). For the sake of simplicity, we chose to employ trapezoidal fuzzy sets to represent both GRel and GDifR. The minimal number of fuzzy sets needed for each component is 2. The resulting fuzzy sets are denoted by GRelSmall, GRelLarge, GDifRSmall and GDifRLarge. Their membership functions, derived manually by the aforementioned technique, are plotted in Figure 8.

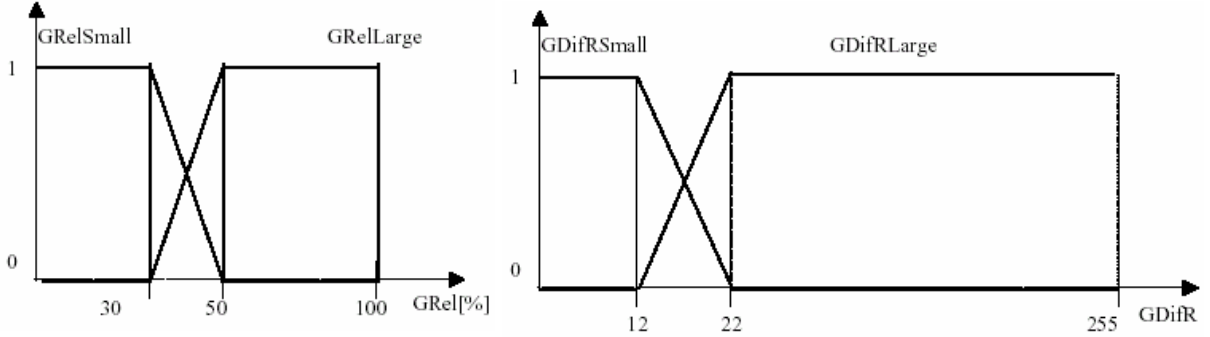


Figure 8. The membership functions of the fuzzy sets *GRelSmall*, *GRelLarge*, *GDifRSmall*, *GDifRLarge* used by the fuzzy if-then rules for the 2-class classification into “sliding bar” and “not sliding bar”

Four fuzzy if-then rules can be defined with these four fuzzy sets. However only one fuzzy rule is of interest for further processing, namely the one having in the consequent the decision “the current color in the fuzzy c-means segmented slice belongs to the sliding bar”. This decision is taken only when the linguistic value of GRel is GRelSmall and the linguistic value of GDifR is GDifRLarge. The corresponding fuzzy rule for the color i in the slice k , denoted as $Color_{ik}$, $i=1,2,3$ and $k=1,2,\dots,10$, is formulated as follows:

R: If $GRel_{ik}$ is GRelSmall **and** $GDifR_{ik}$ is GDifRLarge **then** $Color_{ik}$ is Sliding Bar.

The fuzzy segmentation result of every slice k , $k=1,2,\dots,10$, according to this rule, will be presented as a gray level image, where the luminance component is proportional to the membership degree of $Color_{ik}$ to the class “sliding bar”, resulting after the evaluation of rule R:

$$Y_{2class_segm,k} = (int)(255 \cdot \min(GRelSmall(GRel), GDifRLarge(GDifR))), k = 1,2,\dots,10 \quad (3)$$

(The min operator has been used to implement the “and” connective in the antecedent of the fuzzy rule R). The fuzzy segmentation result is presented in Figure 9(b) for the fuzzy c-means segmented image from Figure 9(a).

Although we could determine now a crisp segmentation by thresholding the membership degrees (luminance values), we consider that keeping a fuzzy segmentation result can be more advantageous for the diagnosis, even for the quantitative image measurements performed in the next step and for the fuzzy expert system decision. We argue our choice through the uncertainty in the human expert decision when prompted to crisply select one of the two classes for the regions in the slices of the ROI.

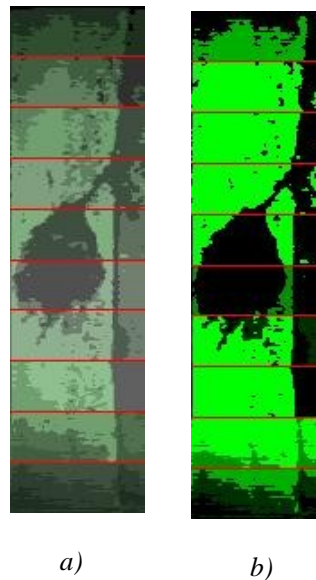


Figure 9. The fuzzy 2-class segmentation result of a ROI: (a) the ROI after fuzzy c-means segmentation in the (R,G,B) color space; (b) the resulting 2-class fuzzy segmented image after applying the fuzzy rule based system

3.3. Quantitative measurements on the object of interest

The aim of this final stage in the image analysis component is to provide the expert system a numerical descriptor about the sliding metal bar in each slice of the ROI. The numerical descriptor will allow the expert system to judge about the status of the bar in the slice, as: good; partially occluded by obstacles (algae, tree branches); totally occluded, etc. A good descriptor to allow the discrimination in such categories is the area of the sliding bar. Having available a 2-class fuzzy segmented image of the sliding bar in each slice of the ROI, we can compute the fuzzy area of the sliding bar in each slice, as the sum of the luminances (that are proportional to the membership degrees of the pixels to the class Sliding bar) of all pixels in the slice:

$$\text{SlidingBarArea}_k = \sum_{i=0}^{W_k-1} \sum_{j=0}^{H_k-1} Y_{2\text{class_segm},k}[i][j] \quad (4)$$

where: (i,j) = the pixel in the relative position (i,j) in the slice k of the ROI; $W_k \times H_k$ = the size of slice k in the ROI.

An even better numerical descriptor to be passed to the expert system is the relative area of the sliding bar in each slice, referenced to the maximal sliding bar area among all the slices in the ROI:

$$\text{RelSlidingBarArea}_k = \frac{\text{SlidingBarArea}_k}{\max_{k=1}^{10} \text{SlidingBarArea}_k} \times 100 \quad (5)$$

4. The fuzzy expert system for upstream dam wall diagnosis

This is the second and last component of the visual-based diagnosis system presented here. A fuzzy logic system was considered more suitable as expert system rather than a crisp solution, considering again the impossibility of a crisp decision about the status of the sliding bar due mainly to the poor quality of the underwater images.

On every evaluation, the fuzzy expert system receives as input the relative area of the sliding bar in a slice of the ROI, $\text{RelSlidingBarArea}_k$, $k=1,2,\dots,10$, as given by equation (5). This crisp input is first fuzzified, then processed through the fuzzy inference engine, based on a set of fuzzy if-then rules and fuzzy sets (the knowledge base of the fuzzy expert system). The processing result is a linguistic message (linguistic diagnostic) describing the status of the sliding bar in the currently processed slice k , $k=1,2,\dots,10$ of the ROI. The most plausible linguistic diagnostic is displayed to the user, without the degree of confidence unless the user asks this information.

4.1. The fuzzy expert system design: fuzzy sets, fuzzy rules and linguistic output values

The following human expert knowledge principles were considered in designing the fuzzy expert system for the diagnosis of the status of the sliding metal bar:

- (a) the maximal area of the sliding bar, $\max_{k=1}^{10} \text{SlidingBarArea}_k$, between all slices, in a ROI of an

underwater image corresponds to the integrity of the bar (i.e. in every ROI, there is at least one slice where the bar is visible); thus, the larger the relative area of the bar per slice, $\text{RelSlidingBarArea}_k$, $k=1,2,\dots,10$, the better the status of the bar in that slice.

(b) if in a slice k , $\text{RelSlidingBarArea}_k$ is close to zero, then in slice k , the bar is either completely occluded by obstacles (tree branches, algae), or the local visibility in the underwater image is too poor to allow the automatic diagnosis.

Any intermediate situations between (a) and (b) correspond to a more or less deterioration/occlusion of the sliding bar.

The above human expert knowledge was gathered as a result of examination of several underwater images of the sliding metal bar. According to these principles, we consider the following linguistic messages provided as diagnostic results by our fuzzy expert system:

Message 1) The status of the bar is good

Message 2) The status of the bar is slightly deteriorated / the bar is slightly occluded by obstacles

Message 3) The status of the bar is highly deteriorated / the bar is highly occluded by obstacles

Message 4) The bar is completely occluded by obstacles or the visibility is too poor for analysis.

The four linguistic messages are the consequences of the four fuzzy if-then rules in the knowledge base of the fuzzy expert system:

R1: If RelSlidingBarArea_k is VerySmall **then** (The sliding bar status in slice k) is Message 4.

R2: If RelSlidingBarArea_k is Small **then** (The sliding bar status in slice k) is Message 3.

R3: If RelSlidingBarArea_k is Medium **then** (The sliding bar status in slice k) is Message 2.

R4: If RelSlidingBarArea_k is Large **then** (The sliding bar status in slice k) is Message 1.

The four fuzzy sets that describe by linguistic values the sliding bar area in each slice: VerySmall, Small, Medium and Large, where again derived making use of the human expert knowledge on the same set of 10 training images used for deriving the fuzzy sets employed in Subsection 3.3. For simplicity, we chose to employ trapezoidal-shaped fuzzy sets. The corresponding membership functions of the four fuzzy sets are represented in Figure 10.

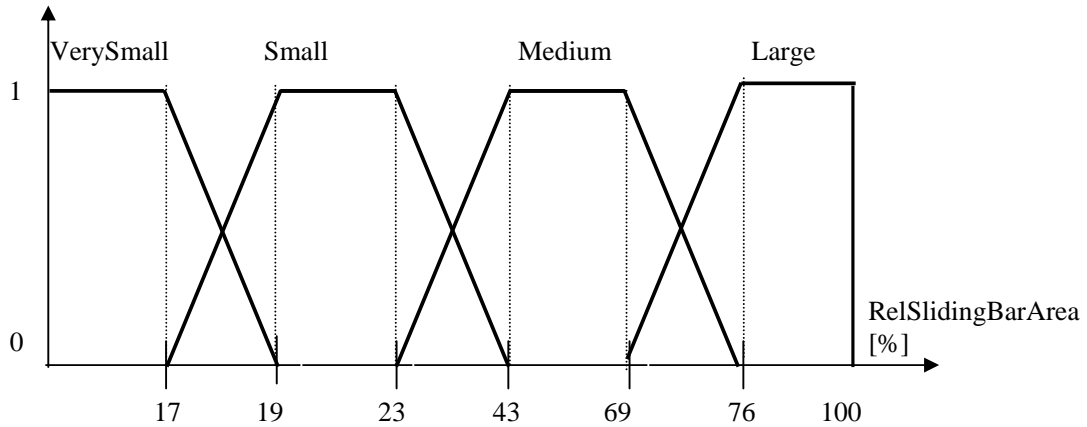


Figure 10. The membership functions for the 4 fuzzy sets in the knowledge base of the fuzzy expert system for the diagnosis of the sliding bar

5. Experimental results

We implemented software the proposed vision-based fuzzy expert system for the diagnosis of the upstream dam walls, based on underwater color image analysis, in C++, as a Windows stand-alone application. The interface allows loading an image to be analyzed, in which it selects automatically the ROI and defines the 10 horizontal slices of the ROI of equal width. The diagnosis is performed when the user presses the corresponding button. As a result, the system generates for each individual slice a linguistic message describing the status of the bar in that region. The fuzzy segmented ROI into sliding metal bar and other scene content (not sliding metal bar) is displayed in the main window of the application, to the right of the message box, to explain the user the decision taken by the fuzzy expert system. The interface and the processing result of our application for an underwater image are presented in Figure 11.

To evaluate the performance of the proposed system, we considered a set of 6 underwater images containing each of them a portion of the sliding bar. These images were obtained as manually selected frames from a video-sequence acquired with an URV in the upstream side of the Tarniā dam on the Some river [11]. As selection criteria we considered the following:

- choose images with different degrees of occlusion of the sliding metal bar with tree branches;
- choose images where the screws are rusted and/or algae are present on the screws;
- choose images where parts of the sliding metal bars are not visible due to the poor illumination in the water

Also the 6 images selected as test set differ noticeably in the average illumination (lighter and darker) and also in the degree of blurring. Although the number of test images is rather small, we consider the test results significant since:

- every ROI extracted from a test image is divided into 10 slices and the diagnosis is done individually on each slice; therefore the actual size of the test set is $6 \times 10 = 60$ test sub-images
- the difference in content, illumination, contrast and blurring between the 6 images is significant (an example can be seen in Figure 2(a) and (b)).

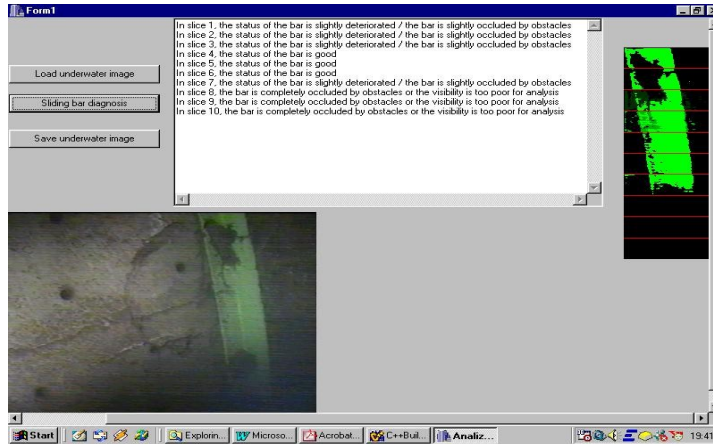


Figure 11. The interface and the processing result of our application for a test underwater image

Since we evaluate the performance of an expert system that is, by its nature, supposed to give diagnosis results as close as possible to the ones of a human expert in the field [12], we set up the following experimental protocol:

(a) We present to a human expert the same ROI examined by the expert system, horizontally divided into the 10 slices considered, however not segmented (neither by fuzzy c-means nor by the fuzzy if-then rule based system).

(b) For each of the 10 horizontal slices, we ask the human expert to give a diagnostic for the sliding metal bar in that slice. The diagnostic can only be selected as one of the 4 possible linguistic messages given by the expert system or at most two of them in case the human cannot decide. In the later case however, we constrain the human expert to choose two messages that have close meanings.

(c) The expert system diagnosis results are compared on each of the 60 test data with the human expert results. Whenever a mismatch between the diagnosis result given by the human expert and the diagnosis result given by the expert system occurs, this is considered an error. The errors are counted both individually on each of the 6 test images and globally, on the test set of 60 sub-images. We denote the 6 test images as $\{TestImg_1, TestImg_2, \dots, TestImg_6\}$. The individual diagnosis error on each image, the average diagnosis error in the test set and the average correct diagnosis rate in the test set are given in Table 2.

Table 2. Individual and average error rates with the proposed fuzzy expert system

<i>Individual diagnosis error [%]</i>						<i>Average diagnosis error [%]</i>	<i>Average correct diagnosis rate [%]</i>
<i>TestImg₁</i>	<i>TestImg₂</i>	<i>TestImg₃</i>	<i>TestImg₄</i>	<i>TestImg₅</i>	<i>TestImg₆</i>		
0	20	10	0	20	0	8.3	91.7

Since according to our knowledge no previous implementations of such a vision-based expert system for the problem of upstream dam wall diagnosis are reported in literature, we will compare the performance of our system only with a somehow similar solution reported in the literature [5], in which the aim is to recognize the underwater cables from seabed images. In that applications, the authors correct report recognition rates about 90%. This is similar to the performance of the vision-based expert system presented in our paper.

6. Conclusions

In this paper we proposed a novel solution towards the automation of underwater hydro-dams monitoring and diagnosis, based on the visual examination of color underwater images of the upstream dam walls acquired with the use of an underwater robot vehicle. Whereas the traditional methods require the human expert to visually examine the underwater images, which is a time-consuming task even in the cases when some upstream walls image mosaic is available, the solution presented here reduces to a larger extent the need for a human expert examination. This goal has been achieved by gathering the human expert knowledge in the field and incorporating it into a fuzzy expert system.

We derived and employed several image analysis techniques suitable to the specific task of sliding metal bars diagnosis as means for numerical data extraction from the underwater images; these numerical data are processed by the fuzzy expert system to obtain the linguistic, human-like, diagnostic results. The performance of the system, evaluated on real test data, proves its good functionality. However we estimate that by the integration of other type of information extracted from the underwater image in the image analysis stage (as e.g. edge information) and through a better learning of the fuzzy sets and rules employed for the we can improve the correct diagnosis rate. This will make the object of our future work.

References:

- [1] Blain, M., "A new generation of underwater robot almost ready to take the plunge", *Recherche-Developement, Institut de Recherche d'Hydro-Quebec* 14 (1): 3, 2001
- [2] J. Batlle, T. Nicosevici, R. Garcia, and M. Carreras, "ROV-aided dam inspection: Practical results," *6th IFAC Conference on Manoeuvring and Control of Marine Crafts (MCMC)*, pp. 309-312, Girona, Spain, 2003
- [3] Takagi, Y., Yoneoka, T., Mori, H., Tsujikawa, A., Saito, T., Karube, K., "Research on dam water level measurement technology by means of a visual sensor", *The Soc. of Environ. Instrum., Control and Automation*, **5(2)**: 179-188, 2000
- [4] Santos-Victor, J., Sentieiro, J. , "The role of vision for underwater vehicles", *Proceedings of the IEEE Symposium on AUV Technology*, pp 28-35, 1994
- [5] Ortiz, A., Simó, M., Oliver, G., "A vision system for an underwater cable tracker", *Machine Vision Applications*, 13(3): 129-140, 2002
- [6] Jain, A. K. , *Foundamentals of Digital Image Processing*, Prentice Hall, New Jersey, 1989
- [7] Lievin, M., Luthon, F., "A hierarchical segmentation algorithm for face analysis. Application to lipreading", *Proc. IEEE Int. Conf. On Multimedia and Expo, 2000. ICME 2000*, 30 July-2 Aug. 2000, New York, USA, vol. 2, pp. 1085 – 1088
- [8] Thitimajshima, P., "A new modified fuzzy c-means algorithm for multispectral satellite images segmentation", *Proc. Geoscience and Remote Sensing Symposium*, Vol. 4, pp. 1684 –1686, 2000
- [9] Park, J., Yae, H., "Analysis of active feature selection in optic nerve data using labeled fuzzy C-means clustering", *Proc. IEEE Int. Conf. on Fuzzy Systems FUZZ-IEEE'02*, Vol. 2, pp.1580 – 1585, 2002
- [10] Bezdek, J. C., *Pattern Recognition with Fuzzy Objective Function Algorithms*, Plenum Press, New York, 1981
- [11] I. Stoian, P. Ungureanu, L. Miclea, M. Gordan, S. Ignat, P. Ridao, "Image Processing Applied to Hydro Plant Surveillance", 28-30 mai 2003, *Proceedings of the 4th Workshop on European Scientific and Industrial Collaboration WESIC 2003*, University of Miskolcz, Ungaria, ISBN 963 661 570 5, vol. II, pp. 389-396
- [12] Kandel, A., *Fuzzy Expert Systems*, CRC Press LLC, 1991